Sustaining fouling resistant membranes: membrane fabrication, characterization and mechanism understanding of demulsification and fouling-resistance

Bing He[1,2], Yajie Ding[2], Jianqiang Wang*[2,3], Zhikan Yao[4], Weihua Qing[4], Yingjie Zhang*[1], Fu Liu*[2,3], Chuyang Y. Tang[4]

1. School of Marine Science and Technology, Sino-Europe Membrane Technology Research Institute, Harbin Institute of Technology, Weihai, 264209, P. R. China;
2. Key Laboratory of Marine Materials and Related Technologies, Ningbo Institute of Materials Technology and Engineering, Chinese Academy of Sciences, Ningbo, 315201, P. R. China;
3. University of Chinese Academy of Sciences, Beijing, 100049, P. R. China;
4. Department of Civil Engineering, The University of Hong Kong, Hong Kong, 999077, P. R. China.

*Please address correspondences to
Dr. Jianqiang Wang (wangjianqiang@nimte.ac.cn), Prof. Yingjie Zhang (zhangyingjie@hit.edu.cn) and Prof. Fu Liu (fu.liu@nimte.ac.cn), Tel.:+86-574-86325963; Fax: +86-574-86325963;

Abstract

Antifouling performance of membranes is the key obstacle limiting their practical applications for oil/water separation. In this study, a sustaining antifouling membrane was fabricated by constructing polydopamine (PDA) micro-/nano-spheres on a polyacrylonitrile (PAN) nanofibrous membrane. The secondary PDA nano-spheres not only strengthened the bonding of primary micro-spheres with the substrate, but also diversified the hierarchical structure and chemistry. The composite showed enhanced superhydrophilicity and underwater superoleophobicity. Permeability of PAN-PDAc membrane was maintained as high as 11666 ± 978 $Lm^{-2}h^{-1}bar^{-1}$ with separation efficiency of higher than 99.9% over a 2-h continuous filtration. This permeability was about 2.7 times of pristine PAN membrane (4260 ± 430 $Lm^{-2}h^{-1}bar^{-1}$). The extrusion and cutting demulsification on the confined space of PAN-PDA surface was proposed. Antifouling mechanism of the superhydrophilic membrane was first theoretically elucidated based on hydration ability and adhesion free energy with recourse to thermal analysis and Derjaguin-Landau-Verwey-Overbeek theory respectively. It was found that PDA micro-/nano-spheres mediated membrane showed strong hydration ability (higher fraction of non-freezable water) and weak adhesion towards toluene (low free energy of adhesion) compared to pristine PAN membrane. These findings would lead to a better understanding of antifouling demulsification mechanism and improved design of sustaining antifouling membranes for oil/water separation.

Key words: Superhydrophilicity; Antifouling; Polydopamine; Nanofibrous membrane; Oil/water separation.

1. Introduction

With the rapid progress of industry and the improvement of people's living standards, more and more oily wastewaters are being produced. Developing economic and effective strategies for treating oily wastewaters is of great importance for both environmental protection and the health of human beings. Compared with conventional strategies for oil/water separation, such as skimming, burning, centrifuge, coagulation and flotation [1, 2], membrane separation is recognized as a more promising method due to its high selectivity, high productivity, energy efficiency and its ability to demulsify the emulsions without applying additional electric field or chemicals [3, 4]. However, the pervasive development of membrane separation is still challenging due to serious fouling issue, e.g., due to oil droplets adhesion, surfactant adsorption, surface wettability/anti-wettability invalidation and microstructure distortion especially during the continuous long term operation. This fouling issue causes rapid decline of flux, separation efficiency and the lifespan of the membrane for separating surfactant-stabilized emulsions [5-7]. In addition, different from common ultrafiltration or microfiltration liquid-solid separation process, the liquid-liquid oil/water separation mechanism via membrane is much less studied. Therefore, it is significant to reveal the fouling mechanism through both theoretical and experimental means. Constructing robust membranes to mitigate fouling for continuous oil/water separation is highly desired.

Generally, improving superwetting property is one of the key methods that can enhance the antifouling performance of the membranes. Up to date, great efforts have been devoted to constructing the superwetting membrane interface based on the integration of hierarchical structure and surface chemistry [8-10]. Based on these considerations, many strategies have been reported, such as electrospray [11-16], surface loading [17-21] and *in situ* structure manipulation [22-24]. From these strategies, we can find that the irregular micro/nano-structure (including organic and inorganic) are usually constructed on the membrane surface. The wettability/anti-wettability was enhanced after the introduction of these micro/nanostructures, such as the electrosprayed polystyrene microspheres [9], polyacrylonitrile microspheres [16] and poly(vinylidene

fluoride) microspheres [14], the surface loaded titanium dioxide or polyethyleneimine microspheres [17, 19, 25] and also the *in situ* formed poly(vinylidene fluoride) microspheres [22, 26] etc. Although the surface structure and chemistry of the membrane were significantly improved by taking advantage of these micro/nano-spheres, their practical applications were limited due to the following considerations: (1) difficult control in the size and morphology of the regular micro/nano-spheres, and (2) low bonding of micro/nano-spheres with the membrane surface, which may cause leaching of spheres and secondary pollution. Therefore, mechanically robust, easily tunable and persistently antifouling membranes are imperative for oil/water separation.

Dopamine (DA), a bio-inspired building block for surface coating, is a nontoxic, nature derived and environmental friendly material, which can be spontaneously self-polymerized on almost any surface to form a uniform coating layer [27]. The formed polydopamine (PDA) layer exhibited several excellent properties including the enhancement of surface hydrophilicity, surface antifouling and surface reactive ability [28-34]. In addition to the forming of two-dimensional PDA surface coating layer, one-dimensional (nanowire and nanofiber [35, 36]) and zero-dimensional (micro/nanosphere [37-39]) PDA can also be synthesized. Specifically, the morphologies (solid or hollow) and size (from 100 nm to 1000 nm) of PDA spheres can be well controlled. In addition, the existence of a large amount of polar functional groups in PDA (e.g., catechol and amine groups) endows the surface with strong affinity with water, which provides stable hydration layer potentially used for direct antifouling applications (e.g., oil/water separation) [40, 41]. However, few reports are endeavored to reveal the fouling mechanism theoretically and experimentally and construct robust membranes with significant mitigation of fouling through combing regularly controlled micro/nanospheres and chemistry.

In this study, a superhydrophilic and underwater superoleophobic composite membrane with enhanced antifouling performance was fabricated by integration of PDA

microspheres and polyacrylonitrile (PAN) nanofibrous membrane. Regular PDA microspheres were firstly synthesized in a water/ethanol mixed solution initiated by ammonia. The obtained PDA microspheres were loaded on the surface of the PAN nanofibrous membrane through a simple gravity filtration process, and then welded in dopamine Tris-HCl solution. The obtained membrane was used for oil-in-water emulsion separation. The fabricated membrane exhibits high permeability, excellent separation efficiency and anti-oil adhesion ability during long-term filtration. The anti-oil adhesion mechanism of this fabricated membrane was theoretically analyzed in a view of hydration ability and Derjaguin-Landau-Verwey-Overbeek (XDLVO) theory. The construction strategy for superwetting membrane and the antifouling mechanism proposed in this study may supply new ideas for oil/water separation applications.

2. Experimental section

2.1 Materials

Polyacrylonitrile (PAN) (average Mw = 150 000) was purchased from Sigma-Aldrich (USA). N,N-dimethylformamide (DMF, ≥99.5%), anhydrous ethanol (≥99.7%), hydrochloric acid (HCl, 36.0%~38.0%) and toluene (≥99.5%) were all purchased from Sinopharm Chemical Reagent Co., Ltd (China). Dopamine hydrochloride (DA, 98%), ammonia solution (25~28%), ethanediol (>99%), n-butanol (99%), tris(hydroxymethyl)aminomethane (≥99.7%), sodium laurylsulfonate (SLS, 99%) and potassium chloride (KCl, ≥99.99%) were all obtained from Aladdin (China).

2.2 Fabrication of PAN nanofibrous base membrane

PAN powder was added to the DMF to form homogeneous PAN/DMF solution with concentration of 6.0 wt% under constant stirring for 6 h at 70 °C. Then, PAN nanofibrous membrane was fabricated through electrospinning according to our previous reported method with some minor changes [42]. Typically, PAN/DMF solution was firstly filled in a syringe with stainless needle (20 G) that was mounted to an electrospinning setup (SS-2535H, Ucalery Co., Ltd. China). Specific details for

electrospun were as follows: the feed rate was kept at 1.13 mL/h, collection distance was 10 cm, rolling speed of the collective metal drum was 80 rpm, the applied voltage was 19 kV with an applied negative voltage (-3 kV) to the collector. After a certain time of electrospun, the obtained PAN nanofibrous membrane was peeled off from the metal drum and heat-pressed at 100 ºC for 4 h before usage.

2.3 Fabrication of the composite nanofibrous membrane

Prior to the fabrication of the composite nanofibrous membrane, PDA microspheres suspensions were firstly synthesized according to the previously reported method [37]. Typically, 0.8 mL of ammonia solution, 80 mL of anhydrous ethanol and 200 mL of deionized water were mixed with gently stirring to get a homogeneous solution. Meanwhile, 20 mL of DA aqueous solution with a concentration of 50 g/L was prepared. The above two solutions were mixed together with continuous stirring for 30 h to synthesis the PDA microspheres suspensions.

The composite membrane was fabricated through the gravity-driven filtration of PDA suspensions (Figure 1). Typically, 15 mL of the synthesized PDA suspensions were filtered through a piece of PAN nanofibrous membrane with a diameter of 4.0 cm under the condition of gravity to get the PDA microspheres loaded nanofibrous membrane. Then the membrane was cleaned with deionized water and dried at room temperature for 24 h (denoted PAN-PDA membrane). After that, the obtained PAN-PDA membrane was immersed into dopamine Tris-HCl solution (2g/L, pH=8.5) for enhancing the integrative stability of the PDA microsphere layer with different time (0 h, 3 h, 6 h, 9 h, 12 h). The corresponding membranes were denoted as PAN-PDAc$_x$, where x denotes the time. Before further use, the membranes were washed with deionized water and ethyl alcohol to remove the residues and dried at room temperature.

2.4 Oil/water separation experiments

Firstly, 0.03 g of SLS was dissolved in 297 mL of deionized water, and then 3.0 mL of toluene was added to the above solution with continuous stirring for 12 h to form the

toluene-in-water emulsion. Separation experiments for the emulsion were carried out under the condition of gravity-driven using a custom-made filtration device. A membrane disk with a diameter of 4 cm was fixed between two quartz tubes. The emulsions were filtrated through this membrane at a constant water head of 10 ± 0.5 cm. Permeability of the membranes was tested at a time interval of 10 min. Recycle experiments were carried out by washing the membrane using deionized water after each 10 min of filtration.

2.5 Characterizations

Morphologies of the membranes are analyzed by a cold field emission scanning electron microscopy (FE-SEM, S4800, Japan) with an applied voltage of 4 kV. Surface tension/dynamic contact angle measuring instrument (DCAT21, China) was employed to characterize the surface tension and wetting performances of the membranes. Intelligent Fourier infrared spectrometer (FTIR, NICOLET 6700, USA) was used to analyze the chemical composition of the membranes. 3D images of membranes were analyzed by confocal laser scanning microscope. Liquid–Liquid Porometer (LLP-1200A, PMI, USA) was employed to measure membrane pore size. Differential scanning calorimeter (DSC214, Germany) was used to analyze the enthalpy change of the membranes. During the measurement process, the hydrated membrane was placed in an open Al crucible. The heating and cooling rate were 10 ºC/min and the temperature range was set from -80 to 100 ºC for all runs. Oil content before and after separation was examined by total organic carbon analyzer (MultiNC2100, Germany). Polarized optical microscopy (BX51, Japan) was used to record the situations of emulsion before and after separation. Porosity (ε) of membranes were calculated by weighing the dry and wet membrane (wetted with n-butanol) through the following equation [43]:

$$\text{Porosity } (\varepsilon)\% = \frac{\frac{m1 - m0}{\rho 1}}{\frac{m1 - m0}{\rho 1} + \frac{m0}{\rho 0}}$$

where, m_1 is the weight of wet membrane wetted with glycol, m_0 is the weight of the dried membrane, ρ_1 is the density of glycol and ρ_0 is the density of polymer.

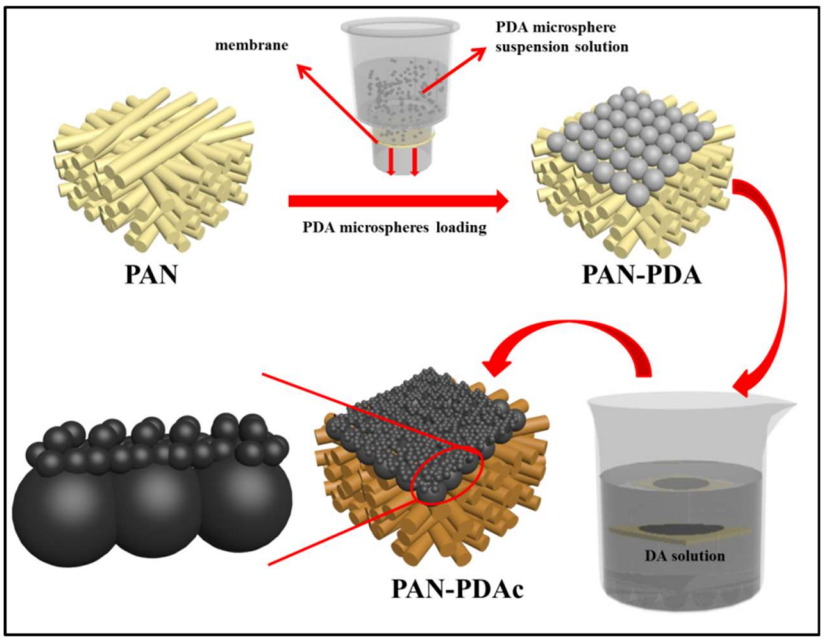

Figure 1. Schematic diagram of the fabrication process for the composite membrane PAN-PDAc.

3. Results and discussion

3.1 Morphologies of the composite membranes

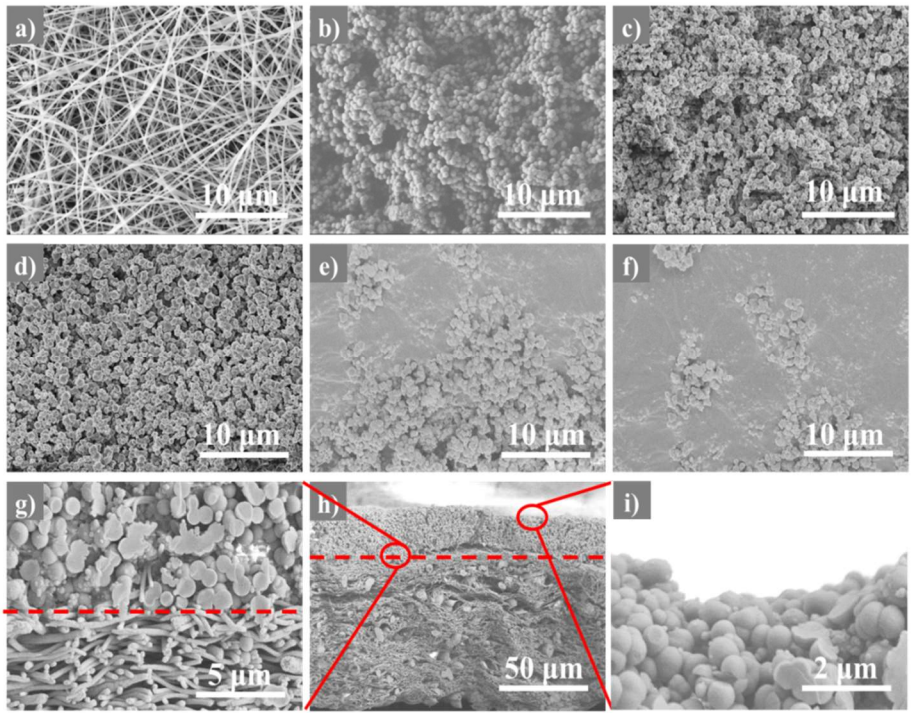

Figure 2. SEM micrographs of a) PAN, b) PAN-PDAc0, c) PAN-PDAc3, d) PAN-PDAc6, e) PAN-PDAc9 and f) PAN-PDAc12; cross-section micrographs of PAN-

PDAc6 (g-i).

Figure 2a presents the morphology of PAN nanofibrous membrane. The results indicate that the membrane was composed of nanofibers with average diameter of 300 nm. After filtration of PDA microsphere suspension, top surface of the nanofibrous membrane was impregnated by the primary PDA microspheres (Figure 2b). However, these PDA microspheres were loosely deposited and can be easily detached from the membrane surface. In order to enhance the integrative stability of the PDA microsphere layer and to further create a hierarchical structure, the PDA loaded PAN nanofibrous membrane was welded by an additional PDA coating through an easy immersion-coating method [27]. As shown in Figure 2c-2f, the pristine smooth microspheres were surrounded by smaller PDA particles. With extending the immersion time from 3 to 6 h, the membrane was gradually covered by the coating. Notably, when the coating time was less than 6 h, the pre-loaded PDA microspheres were firmly welded with each other without sacrificing much of the porosity (Figure S1) and more PDA particles deposited on the microspheres can be found. However, when the coating time was longer than 6 h, more and more surface pores were blocked by the coated PDA layer (Figure 2e-2f). Considering the permeability performance of the nanofibrous membrane, PAN-PDAc$_6$ was used for the following oil/water separation experiments. The cross-section micrographs of PAN-PDAc$_6$ were showed in Figure 2g-2i, and a clear dual layer structure can be found with PDA microspheres deposited on PAN nanofibrous membrane. The constructed PDA microsphere top layer might further enhance the hydrophilicity of the membrane due to the intrinsic hydrophilicity of PDA [44, 45] and enhanced surface roughness.

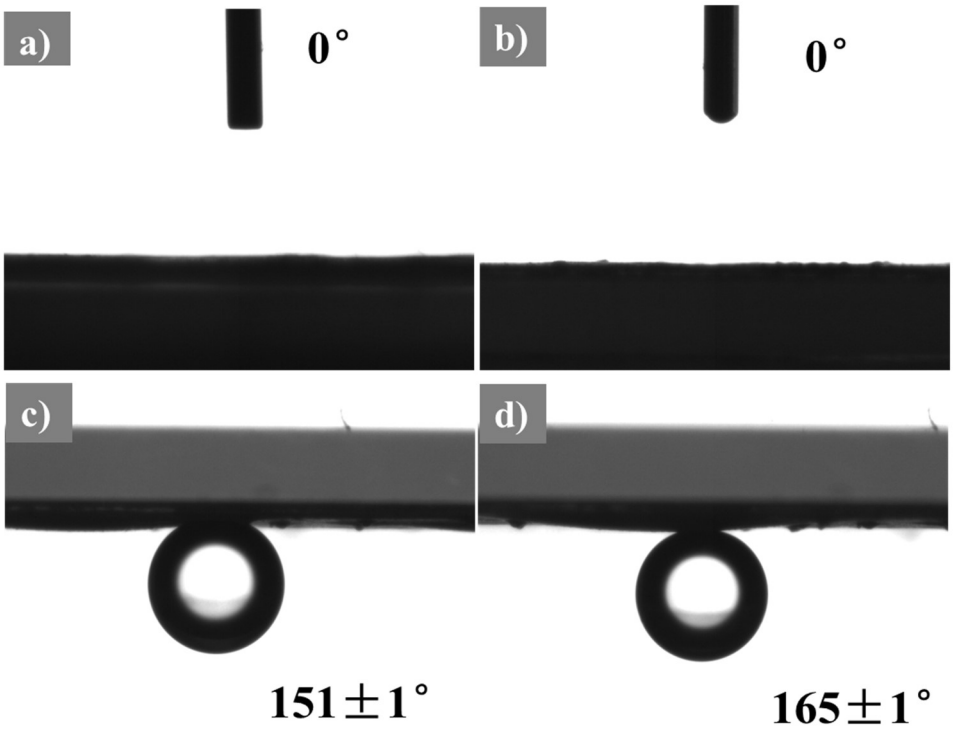

Figure 3. Photographs of the water droplet on PAN (a) and PAN-PDAc6 (b) nanofibrous membrane in air; photographs of the oil droplet on PAN (c) and PDA/PAN (d) nanofbrous membrane under water.

3.2 Wetting performance of the membranes

As wetting property of the membrane plays an important role for its antifouling performance, water contact angles of pristine PAN and PAN-PDAc membranes were tested and the results are showed in Figure 3. Despite the quick water wetting process (about 2.00 s, see supporting information SV1) for 2 μL of water when PAN nanofibrous membrane was used, PAN-$PDAc_6$ membrane exhibited a faster (about 0.12 s, see supporting information SV2) wetting compared to PAN. Underwater oil contact angle (OCA) serves as a more direct parameter to reveal the oleophobic property of the membrane towards oil during filtration process. It is commonly used as an index for antifouling performance of the oil/water separation membranes [16, 46]. As indicated in Figure 3c and d, PAN-PDAc composite membrane showed an enhanced underwater oil contact angle (165±1°) compared to PAN nanofibrous membrane (151±1°), implying better antifouling property. The improved hydrophilicity and oleophobicity

under water might be ascribed to: 1) versatile hierarchical structure composed of primary and secondary PDA micro/nano-spheres, noting that the RSa value (obtained from the CLSM analysis) of the membrane increased from 0.57 μm (PAN membrane) to 2.36 μm (PAN-PDAc$_6$) (Figure 4a-4c); 2) intrinsic hydrophilicity of the PDA attributed to the large amounts of catechol and amine groups (as shown in Figure 4d) [27, 47]; and 3) enhanced capillarity effect due to the multi-scale spheres deposited structure [48, 49].

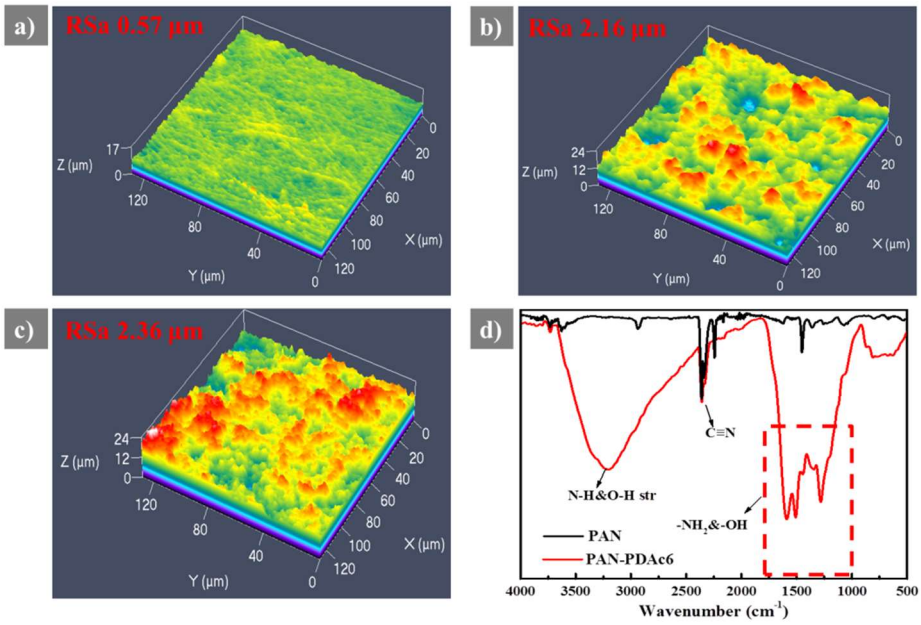

Figure 4. Confocal laser scanning microscope images of PAN (a), PAN-PDAc$_0$ (b) and PAN-PDAc$_6$ (c) membrane; ATR-FTIR spectra of PAN pristine membrane and PAN-PDAc$_6$ membrane (d).

3.3 Sustained separation performance and antifouling mechanism

As shown in Figure 5a, the initial permeability of PAN-PDAc$_6$ nanofibrous membrane for toluene-in-water emulsions was as high as 32256±925 $Lm^{-2}h^{-1}bar^{-1}$, which was 23.3% higher than PAN membrane. This might be mainly due to the enhanced hydrophilicity and capillarity of PAN-PDAc$_6$ membrane compared to PAN membrane (as discussed in section 3.2) [48, 49]. The intuitive results of the emulsions obtained through optical microscopy indicated a great difference before and after filtration, nearly no emulsions

can be found in the filtrate (Figure 5e). Separation efficiency of both PAN and PAN-PDAc membrane can reach up to 99.9%, implying strong demulsification property of nanofibrous membrane (Figure 5a). The size of the emulsion (5-30 μm) was larger than the membrane pore size (0.2-0.3 μm) and can not permeate through the membrane due to the size exclusion [50]. The demulsification mechanism based on physical extrusion was proposed in Figure 5b-5c. The globular oil droplet stabilized by surfactants was distorted in the PAN-PDAc sphere surface or PAN fibrous surface by physical extrusion [51]. The thermodynamic equilibrium was broken with the partial removal and re-arrangement of surfactants on the oil droplet surface [52]. Therefore, the stable emulsion droplets were demulsified, coalesced and repelled by the superhydrophilic nanofibrous or micro-/nano-sphere surface. Besides, the cutting effect of nanofibers as "nanofiber knife" can also induce the deformation of the droplets and non-equilibrium distribution of surfactants, which promotes the demulsification (Figure 5d). Therefore, extrusion distortion in the confined space of PDA microsphere structure was the main demulsification mechanism for PAN-PDAc membrane. However, "nanofiber knife" effect was also contributed to the demulsification performance of the nanofibrous membrane (e.g., PAN nanofibrous membrane).

Actually, rather than the initial separation performance, long-term separation performance of membranes should be of practical significance due to the severe fouling issue. Generally, permeability of the membrane was dramatically reduced just after tens of minutes. As shown in Figure 5a, permeability of the PAN nanofibrous membrane decreased from 26170 ± 860 $Lm^{-2}h^{-1}bar^{-1}$ to 4260 ± 430 $Lm^{-2}h^{-1}bar^{-1}$ after filtration of 2 h. Despite the permeability decline of PAN-$PDAc_6$ (from 32256 ± 925 $Lm^{-2}h^{-1}bar^{-1}$ to 11666 ± 978 $Lm^{-2}h^{-1}bar^{-1}$), permeability of PAN-$PDAc_6$ membrane after 2 h of continuous filtration was 174.8% higher than the corresponding value for the PAN membrane. Considering the initial permeability difference of PAN and PAN-$PDAc_6$ nanofibrous membrane (23.3% of higher compared to PAN-$PDAc_6$ and PAN membrane), the PAN-$PDAc_6$ membrane showed significantly sustained antifouling performance. In addition, the separation performance of PAN-$PDAc_6$ membrane was

reasonably maintained after six filtration cycles (Figure 5f).

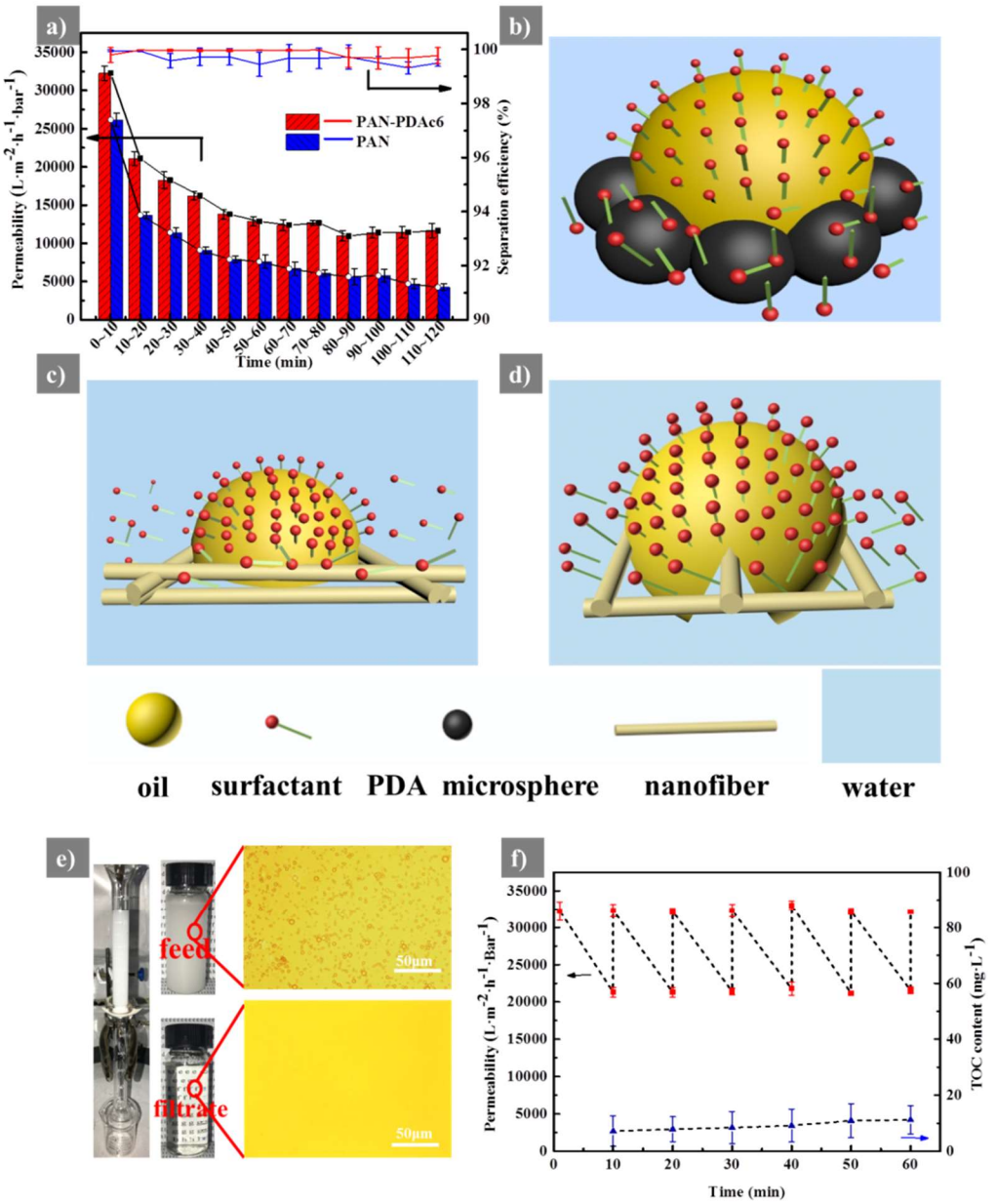

Figure 5. a) Permeability and separation efficiency of PAN and PAN-PDAc$_6$ membrane for toluene-in-water emulsion; Mechanism diagrams of PAN-PDAc$_6$ (b) and PAN (c-d) membrane for demulsification; e) Home-made gravity-driven separation device and the polarized optical microscopy photographs of feed solution emulsion and the filter solution; f) Cycle performance of PAN-PDAc$_6$ membrane.

3.4 Theoretical analysis of antifouling surfaces

The main reason of sustained antifouling performance was attributed to the

hydrophilicity and underwater anti-oil adhesion improvement as discussed in section 3.2. To further understand interaction between the PAN-PDAc$_6$ membrane surface and water, oil foulants, the hydration ability and the interactions between the foulant and membrane were analyzed using thermal analysis method and classic extended Derjaguin-Landau-Verwey-Overbeek (XDLVO) theory respectively.

Water was trapped in the PDA micro-/nano-sphere layer in different states e.g. free water, freezable water and non-freezable water. The closely bound non-freezable water mainly contributed to the mitigation of fouling. Thermal analysis method has been considered as an effective method to analyze the different hydration states of the materials [53-55]. In this method, content of different forms of water in membranes was calculated by the following equations:

$$\mathrm{Ws}(\%) = \frac{\square 1-\mathrm{m0}}{m1} \times 100\% \quad (1)$$

$$\mathrm{Wfs}(\%) = \frac{\Delta \mathrm{Hs}}{\Delta \mathrm{Hw}} \times 100\% \quad (2)$$

$$\mathrm{Wnfs}(\%) = \mathrm{Ws\text{-}Wfs} \quad (3)$$

where m0 is the dry weight before submersion and m1 is the weight of membrane after 24 h hydration, ΔHs is the summation of all the melting enthalpy in the heating trace of wet DSC, ΔHw = 333.5 (J/g). Ws is the swelling ratio, Wfs represents freezable water in the membrane, Wnfs represents non-freezable water (the fraction water that was closely associated with the membrane) content in the membrane.

Results of melting enthalpy of water in PAN and PAN-PDAc$_6$ in the heating trace validated by DSC are shown in Figure 6a-6b. The results indicated that the crystallization peak of PAN-PDAc$_6$ membrane (-20 ^{o}C) shifted to lower temperature compared with PAN membrane (-16 ^{o}C), suggesting different water-membrane interactions. This was confirmed by the quantized results presented in Table 1 that content of non-freezable water in PAN-PDAc$_6$ (34.2%) membrane was 5.5 times higher than pristine PAN membrane (6.0%). As the fraction of non-freezable water was closely associated with the membrane surface to form a hydrogel-like surface, and the water

molecules are difficult to be removed or replaced by the oil due to higher energy barrier, therefore the hydration of PAN-PDAc$_6$ membrane was stronger than PAN membrane, and the PAN-PDAc$_6$ membrane surface exhibited stronger ability to resist oil adhesion than PAN membrane [54].

Table 1. The content of different forms of water in different membranes.

Membrane	Ws (%)	Wfs (%)	Wnfs (%)
PAN	85.0	79.0	6.0
PAN-PDAc$_6$	84.8	50.6	34.2

In addition, the adhesion interaction between the superhydrophilic membrane surface and the oil phase based on the physicochemical interaction energy was analyzed using XDLVO theory for the first time, analogous to foulants adsorption on membrane surface [56]. Here, the oil phase toluene was considered as the foulant during filtration. In this theory, the adhesive strength between the foulant and the hydrated superhydrophilic membrane was represented by the free energy of adhesion ΔG_{132}, where 1 represents the foulant, 2 represents the membrane and 3 represents the water) [56]. Basically, the free interfacial energy is composed of Lifshitz-van der Waals (LW) and acid−base (AB) interaction energies (eq 4.), thus ΔG_{132} can be described as the sum of ΔG_{132}^{LW} and ΔG_{132}^{AB} (eq 5.), and ΔG_{132}^{LW} and ΔG_{132}^{AB} can be calculated by eq 6 and eq 7 respectively [56].

$$\Delta G = \Delta G^{LW} + \Delta G^{AB} \quad (4)$$

$$\Delta G_{132} = \Delta G_{132}^{LW} + \Delta G_{132}^{AB} \quad (5)$$

$$\Delta G_{132}^{LW} = -2(\gamma_3^{LW} + \sqrt{\gamma_1^{LW}\gamma_2^{LW}} - \sqrt{\gamma_1^{LW}\gamma_3^{LW}} - \sqrt{\gamma_2^{LW}\gamma_3^{LW}}) \quad (6)$$

$$\Delta G_{132}^{AB} = -2[\sqrt{\gamma_1^+\gamma_2^-} + \sqrt{\gamma_1^-\gamma_2^+} - \sqrt{\gamma_3^+}(\sqrt{\gamma_1^-} + \sqrt{\gamma_2^-} - \sqrt{\gamma_3^-}) - \sqrt{\gamma_3^-}(\sqrt{\gamma_1^+} + \sqrt{\gamma_2^+} - \sqrt{\gamma_3^+})] \quad (7)$$

where γ^{LW}, γ^+, and γ^- are surface tension parameters. The surface tension parameters can be directly determined by testing three probe liquids (e.g., water, ethylene glycol and diiodomethane) whose surface tension parameters are known.

Table 2. The free interfacial energy parameters of different membranes

Membrane	γ_2^{LW} (mN/m)	γ_2^+ (mN/m)	γ_2^- (mN/m)	ΔG_{132}^{LW} (mJ/m^2)	ΔG_{132}^{AB} (mJ/m^2)	ΔG_{132} (mJ/m^2)
PAN	45.98	-2.55	8.18	-2.80	-45.7	-48.46
PAN-PDAc6	46.57	-3.06	10.52	-2.80	-40.82	-43.62

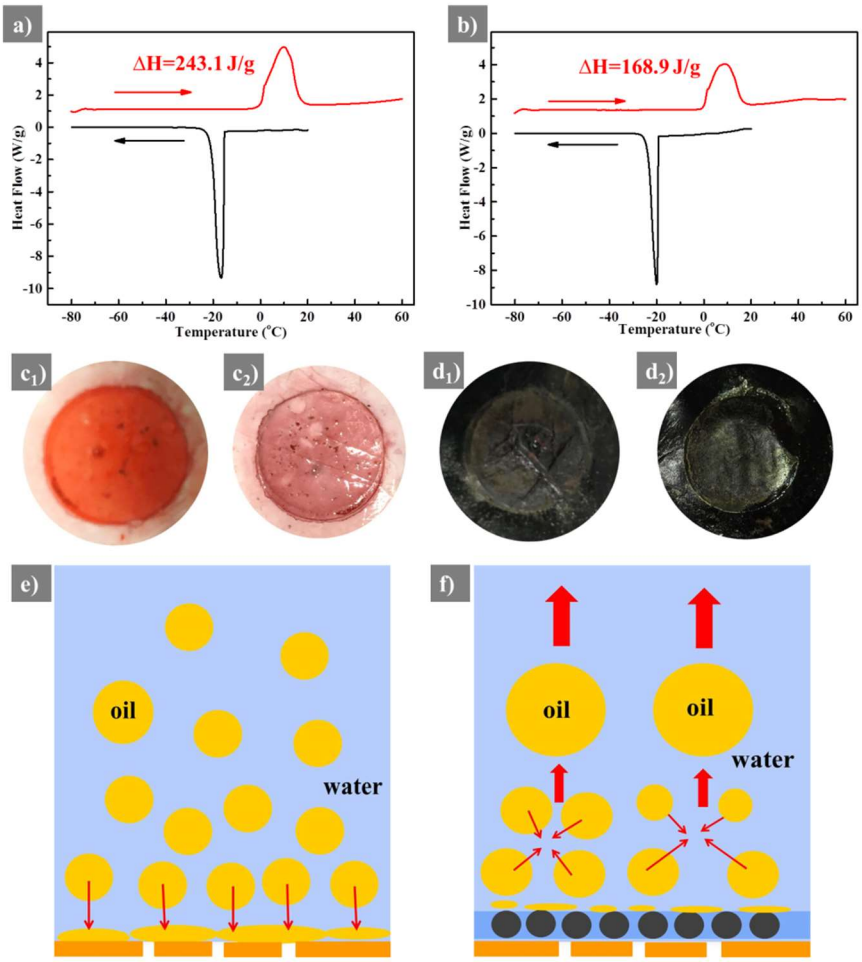

Figure 6. DSC thermograms of water saturated PAN (a) and PAN-PDAc$_6$ (b) membrane; Photos of PAN membrane after 120 min of filtration for toluene-in-water emulsion before (c_1) and after (c_2) rinsing; Photos of the PAN-PDAc$_6$ after 120 min of separation for toluene-in-water emulsion before (d_1) and after (d_2) rinsing; Schematic diagrams of PAN (e) and PAN-PDAc$_6$ (f) membrane for the separation of oil-water emulsion.

The calculated adhesion free energies of PAN and PAN-PDAc$_6$ membrane between toluene are shown in Table 2. As results indicated that adhesion free energy (ΔG_{132}) between toluene and PAN membrane was -48.46 mJ/m^2. However, the adhesion free energy between toluene and PAN-PDAc$_6$ membrane was -43.62 mJ/m^2, indicating that the attachment strength between toluene and PAN-PDAc$_6$ membrane was smaller than the strength between toluene and PAN membrane. The visual results showed that a thick layer of colored oil was firmly adhered onto PAN nanofibrous membrane surface after 120 min of filtration, and the adhered oils were unable to be removed from membrane surface by rinsing (Figure 6c$_1$ and c$_2$). As a control, there is almost no oil adhered on PAN-PDAc$_6$ membrane even after 120 min continuous filtration, and the residual oil can be easily washed away by simple water rinsing (Figure 6d$_1$ and d$_2$). This comparison clearly shows that PAN-PDAc$_6$ membrane with PDA mediated micro-/nano-spheres possessed excellent oil antifouling performance during continuous filtration. A clear floating oil layer can be found on the feed solution after 120 min of separation (Figure S2). Schematic diagrams of oil/water separation are shown in Figure 6e-6f. When PAN nanofibrous membrane was used for oil/water separation, oils trend to adhere on the membrane surface due to the weak hydration ability and high adhesion free energy. However, PAN-PDAc$_6$ membrane presented better anti-adhesion property towards oils benefitting from its strong hydration ability and low adhesion free energy.

4. Conclusion

In this study, PAN-PDAc composite membrane with sustaining fouling resistance was fabricated through embedding PDA micro-/nano-spheres on PAN nanofibrous substrate. The micro-/nano-spheres mediated composite membrane showed enhanced superhydrophilicity and underwater superoleophobicity. The secondary PDA nano-spheres not only consolidate the bonding of primary micro-spheres with the substrate, but also diversify the hierarchical structure and chemistry. The hydration ability and adhesion free energy were used to elucidate the oil antifouling mechanism of the membrane theoretically for the first time. Permeability of PAN-PDAc membrane was

maintained as high as 11666 ± 978 $Lm^{-2}h^{-1}bar^{-1}$ even after continuous filtration of toluene-in-water emulsions for 2 h, which was about 2.7 times compared to PAN membrane (4260 ± 430 $Lm^{-2}h^{-1}bar^{-1}$). Overall, these finding have great implications for constructing sustaining fouling resistant membranes and understanding demulsification and antifouling mechanism in oil/water separation.

Acknowledgements

This work is financially supported by National Key R&D Program of China (2017YFB0309600), National Nature Science Foundation of China (51703233, 5161101025), Youth Innovation Promotion Association of Chinese Academy of Science (2014258) and Nature Science Foundation of Ningbo (2018A610026). The authors also acknowledge the partial financial support from the NSFC/RGC Joint Research Scheme sponsored by the Research Grants Council of Hong Kong and the National Natural Science Foundation of China (N_HKU706/16).

References

[1] Z.L. Chu, Y.J. Feng, S. Seeger, Oil/water separation with selective superantiwetting/superwetting surface materials, Angew. Chem., Int. Ed., 54 (2015) 2328-2338.

[2] B. Wang, W. Liang, Z. Guo, W. Liu, Biomimetic super-lyophobic and super-lyophilic materials applied for oil/water separation: A new strategy beyond nature, Chem. Soc. Rev., 44 (2015) 336-361.

[3] Y. Zhu, D. Wang, L. Jiang, J. Jin, Recent progress in developing advanced membranes for emulsified oil/water separation, NPG Asia Mater., 6 (2014) e101-e101.

[4] L. Hou, N. Wang, J. Wu, Z. Cui, L. Jiang, Y. Zhao, Bioinspired superwettability electrospun micro/nanofibers and their applications, Adv. Funct. Mater., 28 (2018) 1801114.

[5] H.-J. Li, Y.-M. Cao, J.-J. Qin, X.-M. Jie, T.-H. Wang, J.-H. Liu, Q. Yuan, Development and characterization of anti-fouling cellulose hollow fiber uf membranes for oil–water separation, J. Membr. Sci., 279 (2006) 328-335.

[6] D. Rana, T. Matsuura, Surface modifications for antifouling membranes, Chem. Rev., 110 (2010) 2448-2471.

[7] Y. Zhu, J. Wang, F. Zhang, S. Gao, A. Wang, W. Fang, J. Jin, Zwitterionic nanohydrogel grafted pvdf membranes with comprehensive antifouling property and superior cycle stability for oil-in-water emulsion separation, Adv. Funct. Mater., 28 (2018) 1804121.

[8] X. Gao, L. Jiang, Water-repellent legs of water striders, Nature, 432 (2004) 36.

[9] L. Jiang, Y. Zhao, J. Zhai, A lotus-leaf-like superhydrophobic surface: A porous

microsphere/nanofiber composite film prepared by electrohydrodynamics, Angew. Chem., Int. Ed., 43 (2004) 4338-4341.
[10] Q. Ma, H. Cheng, A.G. Fane, R. Wang, H. Zhang, Recent development of advanced materials with special wettability for selective oil/water separation, Small, 12 (2016) 2186-2202.
[11] J. Ge, J. Zhang, F. Wang, Z. Li, J. Yu, B. Ding, Superhydrophilic and underwater superoleophobic nanofibrous membrane with hierarchical structured skin for effective oil-in-water emulsion separation, J. Mater. Chem. A, 5 (2017) 497-502.
[12] E.J. Lee, B.J. Deka, J. Guo, Y.C. Woo, H.K. Shon, A.K. An, Engineering the re-entrant hierarchy and surface energy of pdms-pvdf membrane for membrane distillation using a facile and benign microsphere coating, Environ. Sci. Technol. Lett., 51 (2017) 10117-10126.
[13] H. Attia, D.J. Johnson, C.J. Wright, N. Hilal, Robust superhydrophobic electrospun membrane fabricated by combination of electrospinning and electrospraying techniques for air gap membrane distillation, Desalination, 446 (2018) 70-82.
[14] J. Wu, Y. Ding, J. Wang, T. Li, H. Lin, J. Wang, F. Liu, Facile fabrication of nanofiber- and micro/nanosphere-coordinated pvdf membrane with ultrahigh permeability of viscous water-in-oil emulsions, J. Mater. Chem. A, 6 (2018) 7014-7020.
[15] Z. Zhu, Z. Liu, L. Zhong, C. Song, W. Shi, F. Cui, W. Wang, Breathable and asymmetrically superwettable janus membrane with robust oil-fouling resistance for durable membrane distillation, J. Membr. Sci., 563 (2018) 602-609.
[16] J. Ge, D. Zong, Q. Jin, J. Yu, B. Ding, Biomimetic and superwettable nanofibrous skins for highly efficient separation of oil-in-water emulsions, Adv. Funct. Mater., 28 (2018) 1705051.
[17] H.-C. Yang, K.-J. Liao, H. Huang, Q.-Y. Wu, L.-S. Wan, Z.-K. Xu, Mussel-inspired modification of a polymer membrane for ultra-high water permeability and oil-in-water emulsion separation, J. Mater. Chem. A, 2 (2014) 10225.
[18] H. Shi, Y. He, Y. Pan, H. Di, G. Zeng, L. Zhang, C. Zhang, A modified mussel-inspired method to fabricate tio2 decorated superhydrophilic pvdf membrane for oil/water separation, J. Membr. Sci., 506 (2016) 60-70.
[19] Z. Xiong, H. Lin, Y. Zhong, Y. Qin, T. Li, F. Liu, Robust superhydrophilic polylactide (pla) membranes with a tio2 nano-particle inlaid surface for oil/water separation, J. Mater. Chem. A, 5 (2017) 6538-6545.
[20] Y. Liao, M. Tian, R. Wang, A high-performance and robust membrane with switchable super-wettability for oil/water separation under ultralow pressure, J. Membr. Sci., 543 (2017) 123-132.
[21] J. Wang, L.a. Hou, K. Yan, L. Zhang, Q.J. Yu, Polydopamine nanocluster decorated electrospun nanofibrous membrane for separation of oil/water emulsions, J. Membr. Sci., 547 (2018) 156-162.
[22] W. Zhang, Z. Shi, F. Zhang, X. Liu, J. Jin, L. Jiang, Superhydrophobic and superoleophilic pvdf membranes for effective separation of water-in-oil emulsions with high flux, Adv. Mater., 25 (2013) 2071-2076.
[23] M. Huang, Y. Si, X. Tang, Z. Zhu, B. Ding, L. Liu, G. Zheng, W. Luo, J. Yu, Gravity driven separation of emulsified oil–water mixtures utilizing in situ polymerized superhydrophobic and superoleophilic nanofibrous membranes, J. Mater. Chem. A, 1 (2013) 14071.
[24] M. Tao, L. Xue, F. Liu, L. Jiang, An intelligent superwetting pvdf membrane showing switchable transport performance for oil/water separation, Adv. Mater., 26 (2014) 2943-2948.
[25] H. Shi, Y. He, Y. Pan, H.H. Di, G.Y. Zeng, L. Zhang, C.L. Zhang, A modified mussel-inspired method to fabricate tio2 decorated superhydrophilic pvdf membrane for oil/water separation, J. Membr. Sci., 506

(2016) 60-70.
[26] W. Zhang, Y. Zhu, X. Liu, D. Wang, J. Li, L. Jiang, J. Jin, Salt-induced fabrication of superhydrophilic and underwater superoleophobic paa-g-pvdf membranes for effective separation of oil-in-water emulsions, Angew. Chem., Int. Ed., 53 (2014) 856-860.
[27] H. Lee, S.M. Dellatore, W.M. Miller, P.B. Messersmith, Mussel-inspired surface chemistry for multifunctional coatings, Science, 318 (2007) 426-430.
[28] S. Kasemset, A. Lee, D.J. Miller, B.D. Freeman, M.M. Sharma, Effect of polydopamine deposition conditions on fouling resistance, physical properties, and permeation properties of reverse osmosis membranes in oil/water separation, J. Membr. Sci., 425 (2013) 208-216.
[29] L. Huang, J.T. Arena, S.S. Manickam, X. Jiang, B.G. Willis, J.R. McCutcheon, Improved mechanical properties and hydrophilicity of electrospun nanofiber membranes for filtration applications by dopamine modification, J. Membr. Sci., 460 (2014) 241-249.
[30] Y. Li, Y. Su, X. Zhao, X. He, R. Zhang, J. Zhao, X. Fan, Z. Jiang, Antifouling, high-flux nanofiltration membranes enabled by dual functional polydopamine, ACS Appl. Mater. Interfaces, 6 (2014) 5548-5557.
[31] Y. Xiang, F. Liu, L. Xue, Under seawater superoleophobic pvdf membrane inspired by polydopamine for efficient oil/seawater separation, J. Membr. Sci., 476 (2015) 321-329.
[32] H. Guo, Y. Deng, Z. Tao, Z. Yao, J. Wang, C. Lin, T. Zhang, B. Zhu, C.Y. Tang, Does hydrophilic polydopamine coating enhance membrane rejection of hydrophobic endocrine-disrupting compounds?, Environ. Sci. Technol. Lett., 3 (2016) 332-338.
[33] H.-C. Yang, R.Z. Waldman, M.-B. Wu, J. Hou, L. Chen, S.B. Darling, Z.-K. Xu, Dopamine: Just the right medicine for membranes, Adv. Funct. Mater., 28 (2018) 1705327.
[34] J. Wang, Z. Wu, T. Li, J. Ye, L. Shen, Z. She, F. Liu, Catalytic pvdf membrane for continuous reduction and separation of p -nitrophenol and methylene blue in emulsified oil solution, Chem. Eng. J., 334 (2018) 579-586.
[35] X. Yu, H. Fan, L. Wang, Z. Jin, Formation of polydopamine nanofibers with the aid of folic acid, Angew. Chem., Int. Ed., 53 (2014) 12600-12604.
[36] J. Xue, W. Zheng, L. Wang, Z. Jin, Scalable fabrication of polydopamine nanotubes based on curcumin crystals, ACS Biomater. Sci. Eng., 2 (2016) 489-493.
[37] K. Ai, Y. Liu, C. Ruan, L. Lu, G.M. Lu, Sp2 c-dominant n-doped carbon sub-micrometer spheres with a tunable size: A versatile platform for highly efficient oxygen-reduction catalysts, Adv. Mater., 25 (2013) 998-1003.
[38] X. Jiang, Y. Wang, M. Li, Selecting water-alcohol mixed solvent for synthesis of polydopamine nano-spheres using solubility parameter, Sci. Rep., 4 (2014) 6070.
[39] J. Wang, X. Pei, G. Liu, J. Bai, Y. Ding, J. Wang, F. Liu, Gravity-driven catalytic nanofibrous membrane with microsphere and nanofiber coordinated structure for ultrafast continuous reduction of 4-nitrophenol, J. Colloid Interface Sci., 538 (2019) 108-115.
[40] H.-C. Yang, J. Luo, Y. Lv, P. Shen, Z.-K. Xu, Surface engineering of polymer membranes via mussel-inspired chemistry, J. Membr. Sci., 483 (2015) 42-59.
[41] S. Gao, J. Sun, P. Liu, F. Zhang, W. Zhang, S. Yuan, J. Li, J. Jin, A robust polyionized hydrogel with an unprecedented underwater anti-crude-oil-adhesion property, Adv. Mater., 28 (2016) 5307-5314.
[42] J. Wang, H. Guo, Z. Yang, Y. Mei, C.Y. Tang, Gravity-driven catalytic nanofibrous membranes prepared using a green template, J. Membr. Sci., 525 (2017) 298-303.
[43] J. Wang, Y. Wu, Z. Yang, H. Guo, B. Cao, C.Y. Tang, A novel gravity-driven nanofibrous membrane

for point-of-use water disinfection: Polydopamine-induced in situ silver incorporation, Sci Rep, 7 (2017) 2334.
[44] L. Huang, S. Zhao, Z. Wang, J. Wu, J. Wang, S. Wang, In situ immobilization of silver nanoparticles for improving permeability, antifouling and anti-bacterial properties of ultrafiltration membrane, J. Membr. Sci., 499 (2016) 269-281.
[45] J. Wang, H. Guo, X. Shi, Z. Yao, W. Qing, F. Liu, C.Y. Tang, Fast polydopamine coating on reverse osmosis membrane: Process investigation and membrane performance study, J Colloid Interface Sci, 535 (2019) 239-244.
[46] L. Li, Z. Liu, Q. Zhang, C. Meng, T. Zhang, J. Zhai, Underwater superoleophobic porous membrane based on hierarchical tio2 nanotubes: Multifunctional integration of oil–water separation, flow-through photocatalysis and self-cleaning, J. Mater. Chem. A, 3 (2015) 1279-1286.
[47] Q. Wei, F. Zhang, J. Li, B. Li, C. Zhao, Oxidant-induced dopamine polymerization for multifunctional coatings, Polym. Chem., 1 (2010) 1430-1433.
[48] F. Li, Z. Wang, S. Huang, Y. Pan, X. Zhao, Flexible, durable, and unconditioned superoleophobic/superhydrophilic surfaces for controllable transport and oil-water separation, Adv. Funct. Mater., 28 (2018) 1706867.
[49] J. Ge, Q. Jin, D. Zong, J. Yu, B. Ding, Biomimetic multilayer nanofibrous membranes with elaborated superwettability for effective purification of emulsified oily wastewater, ACS Appl. Mater. Interfaces, 10 (2018) 16183-16192.
[50] S.L. Huang, R.H.A. Ras, X.L. Tian, Antifouling membranes for oily wastewater treatment: Interplay between wetting and membrane fouling, Curr. Opin. Colloid Interface Sci., 36 (2018) 90-109.
[51] T. Darvishzadeh, V.V. Tarabara, N.V. Priezjev, Oil droplet behavior at a pore entrance in the presence of crossflow: Implications for microfiltration of oil–water dispersions, J. Membr. Sci., 447 (2013) 442-451.
[52] V. Carpintero-Tepole, E. Brito-de la Fuente, B. Torrestiana-Sánchez, Microfiltration of oil in water (o/w) emulsions: Effect of membrane microstructure and surface properties, Chem. Eng. Res. Des., 126 (2017) 286-296.
[53] D.G. Pedley, B.J. Tighe, Water binding properties of hydrogel polymers for reverse osmosis and related applications, Br. Polym. J., 11 (1979) 130-136.
[54] V. Gun'ko, I. Savina, S. Mikhalovsky, Properties of water bound in hydrogels, Gels, 3 (2017) 37.
[55] F. Zhao, X. Zhou, Y. Shi, X. Qian, M. Alexander, X. Zhao, S. Mendez, R. Yang, L. Qu, G. Yu, Highly efficient solar vapour generation via hierarchically nanostructured gels, Nat. Nanotechnol., 13 (2018) 489-495.
[56] L. Li, Z. Wang, L.C. Rietveld, N. Gao, J. Hu, D. Yin, S. Yu, Comparison of the effects of extracellular and intracellular organic matter extracted from microcystis aeruginosa on ultrafiltration membrane fouling: Dynamics and mechanisms, Environ. Sci. Technol., 48 (2014) 14549-14557.